Journal of Applied Electrochemistry (2006) 36:433–439
DOI 10.1007/s10800-005-9088-5

Oxidation of *p*-methoxyphenol on SnO_2–Sb_2O_5 electrodes: Effects of electrode potential and concentration on the mineralization efficiency

C. BORRÁS*, C. BERZOY, J. MOSTANY and B.R. SCHARIFKER
Departamento de Química, Universidad Simón Bolívar, Apartado 89000, Caracas, 1080A, Venezuela
*(*author for correspondence, e-mail: cborras@usb.ve)*

Received 18 April 2005; accepted in revised form 25 October 2005

Key words: electrocatalysis, metal oxide anode, oxidation of organics, *p*-methoxyphenol

Abstract

The oxidation of *p*-methoxyphenol in aqueous solution on antimony-doped tin oxide has been studied, and the effects of applied potential and initial PMP concentration upon the oxidation rate have been identified. The concentration decay of PMP during its electrooxidation follows first-order reaction kinetics. Analysis solution during electrolysis using UV–Vis spectroscopy revealed that under some experimental conditions partial oxidation of PMP occurs. The principal products were p-benzoquinone and aliphatic (maleic and oxalic) acids. The Faradaic efficiencies for oxidation at different applied potentials were determined from the UV–Vis spectra obtained. It is shown that production of CO_2 was very low at potentials below 2.3 V with respect to the saturated calomel electrode, and that at more positive potentials mineralization to CO_2 decreased as the concentration of PMP in solution increased.

1. Introduction

Electrochemical methods may be used for the partial or total degradation of phenols present in industrial effluents for which treatment by traditional decontaminating methods is not practical. Thus oxidation of phenols by oxygen transfer from solvent water to yield oxidation products has been the chief goal of many laboratories [1–10]. As discussed elsewhere [11–13] OH species originating from the solvent participate in the oxygen transfer process. The reactions taking place on the electrode surface may be written as follows:

$$M[\,] + H_2O \rightarrow M[OH] + H^+ + e^- \quad (1)$$

$$M[OH] + H_2O \rightarrow M[\,] + O_2 + 3H^+ + 3e^- \quad (2)$$

$$M[OH] + R \rightarrow M[\,] + RO + H^+ + e^- \quad (3)$$

where M[ ] corresponds to an adsorption site on the surface and R is the organic compound being oxidized. Due to concurrent oxidation of water and the organic compound through pathways (1)–(2) and (1)–(3), evaluation of the electrocatalytic activity of the surface towards oxidation of the organic needs establishing the distinct contributions of both processes to the total current.

The electrochemical reactivity of each organic compound, as well as the reaction mechanism, depend on the anode material used. On noble metal electrodes, oxidation of phenols is inhibited by deposition of polymer films on the surface [14, 15], whereas full oxidation to CO_2 has been frequently observed on other surfaces such as boron-doped diamond [16–21] or metal oxide electrodes [22, 23]. Two limiting paths have been proposed for oxygen transfer to organic compounds on these electrodes, either from adsorbed hydroxyl radicals generated by discharge of water, or from the superoxide formed during incorporation of oxygen from adsorbed hydroxyl radicals into the metal oxide crystal lattice [24, 25]. The first case has been observed on diamond, SnO_2 and PbO_2 electrodes, where fully oxidized products were obtained, whereas selective oxidation of organics through formation of superoxide has been observed on IrO_2 and RuO_2 [26].

In the present work we have studied the oxidation of *p*-methoxyphenol (PMP) on antimony-doped tin oxide (Sb–SnO_2) electrodes; the effects of electrode potential and PMP initial concentration on oxidation kinetics and mineralization efficiencies have been determined. Analysis of solutions during electrolysis was carried out by UV–Vis spectroscopy and high performance liquid chromatography (HPLC). The results obtained show that although the oxidation rates of the intermediates formed during the reaction increase at increasingly positive electrode potentials, the efficiency for CO_2 generation decreases. PMP oxidation follows first order kinetics and increasing the PMP concentration enhances formation of BQ in solution; at concentrations of PMP close to 0.1 M the oxidation rate of PMP decreases due to formation of a film on the electrode surface.

2. Experimental

Working electrodes were prepared from antimony-doped tin oxide thin films deposited on glass substrate, with sheet resistance of $\sim 70\ \Omega\ cm^{-1}$, obtained from PPG industries, Inc. Electrical contacts to silver wires were realized with silver-loaded epoxy, and these assemblies were isolated with Teflon® thermally shrinkable tubing in order to expose ca. 1 cm^2 of Sb–SnO_2 surface to the solution. Measurements were conducted using a three-compartment glass cell, maintaining separated the solution in the working electrode compartment with a glass frit from that contacting the 2.2 cm^2 platinum wire used as secondary electrode, the saturated calomel electrode (SCE) used as reference. All potentials are reported with respect to the SCE unless otherwise stated. Reagents were of analytical grade (Aldrich or Sigma) and all solutions were prepared with distilled and ultrafiltered (Nanopure®) water.

Electrolysis at constant potentials were carried out with an EG&G PAR model 273 potentiostat, using working electrodes as described above and platinum gauze with larger geometrical surface area as counter electrode. The working electrode compartment was filled for these experiments with 20 ml of phenol-containing solution.

Variation of the PMP concentration during electrolysis at constant potential was determined from UV–Vis spectra. Spectroscopic data were obtained with a Hewlett-Packard 8452A diode-array spectrometer under HP 89531 MS-DOS UV/Vis Operating Software, from 100 μl aliquots sampled from the electrolysis cell at different times, and diluted to 10 ml with water. The experimental UV–Vis spectra thus obtained were deconvoluted into Lorentzian bands with Jandel Peakfit v. 3.0. The concentrations of the different compounds present in solution were determined using the Lambert–Beer law, with molar absorption coefficients ε obtained from calibration curve data at the wavelengths of maximum absorption for each compound, as reported in Table 1.

Liquid chromatography was carried out with a Water Association HPLC system composed of a Model M6000A pump, a Ryhodine injector, a Model 484 UV detector and a Model 745B data recorder. A Nova-Pack C18, 3.9×150 mm column was used for phenol and quinones detection, with 60/40 methanol/water solution as mobile phase, at 0.8 ml min^{-1} flow rate and 254 nm UV–Vis detection. Aliphatic acids (AA) were analyzed with an Aminex HPX-87, 7.8×300 mm column, using 8×10^{-4} M sulfuric acid aqueous solution as mobile phase at 0.5 ml min^{-1} flow rate, with detection at 210 nm.

Table 1. Molar absorption coefficients ε of species in solution

Compound	λ/nm	$10^{-3}\ \varepsilon/cm^{-1}\ M^{-1}$
p-methoxyphenol (*PMP*)	222	7.8
p-benzoquinone (*BQ*)	248	19.7
maleic acid (*MA*)	210	13.8

3. Results and discussion

3.1. *Electrode potential effects*

Figure 1 shows a cyclic voltammogram of the Sb–SnO_2 electrode in 0.001 M PMP and 0.1 M Na_2SO_4 solution. Oxidation currents are observed at potentials more positive than ca. 0.8 V (SCE), reaching a plateau between 1.4 and 1.6 V (SCE), corresponding to the oxidation of PMP to the methoxyphenoxy radical. The current then increases continuously at more positive potentials due to the onset of oxygen evolution. At potentials sufficiently positive for water decomposition, i.e., E > 1.60 V (SCE), the electrogenerated hydroxyl radical transfers oxygen to the organic compound. In contrast, PMP undergoes oxidation through direct electron transfer on the Sb_2O_3–SnO_2 surface at lower potentials, E < 1.60 V (SCE), resulting in electrode fouling due to formation of oligomers resulting from the coupling of methoxyphenoxy radicals generated during the process. Thus potentials sufficiently positive for water descomposition were maintained throughout the experiments reported in this work.

The kinetics of oxidation of PMP on SnO_2 electrode was followed with UV–Vis spectra. Figure 2 shows the deconvolution of a spectrum obtained during electrolysis at constant potential in 0.001 M PMP + 0.1 M Na_2SO_4 aqueous solution. Bands I and II are associated to PMP. Appearance of coloration in the solution and the position of band III in the spectrum, suggest the formation of a quinoid compound during electrolysis maybe p-benzoquinone (BQ) [27, 28]. A fourth band emerges after the passage of large amounts of electric charge; this fourth band is associated to the presence of aliphatic acids (AA) in solution [1, 4, 13, 21].

In order to verify the results obtained from UV–Vis spectroscopy (Figure 2), samples of a 0.1 mM PMP in aqueous 0.1 M Na_2SO_4 solution electrolyzed at 2.5 V were analyzed with HPLC. The results show a series of low amplitude signals corresponding to aromatic compounds, with a single significant signal corresponding to BQ, as verified using the pure compound, with results coincident with those obtained from UV–Vis spectroscopy as described above. HPLC analysis of aliphatic acids after different reaction times showed the presence of maleic and oxalic acids for short time of electrolysis; however, for long times of electrolysis (above 3500 s) only maleic acid was detected. Thus band IV in Figure 2 for long time contains predominantly the contributions of maleic acid.

From these results the sequence of reactions leading to the mineralization of PMP to CO_2 may be represented as:

$$\mathrm{PMP} \xrightarrow{k_1} \mathrm{BQ} \xrightarrow{k_2} \mathrm{AA} \xrightarrow{k_3} \mathrm{CO_2} \qquad (4)$$

The overall rate of the chemical transformation is determined by the slowest step in the series of elementary processes including mass transport to the electrode,

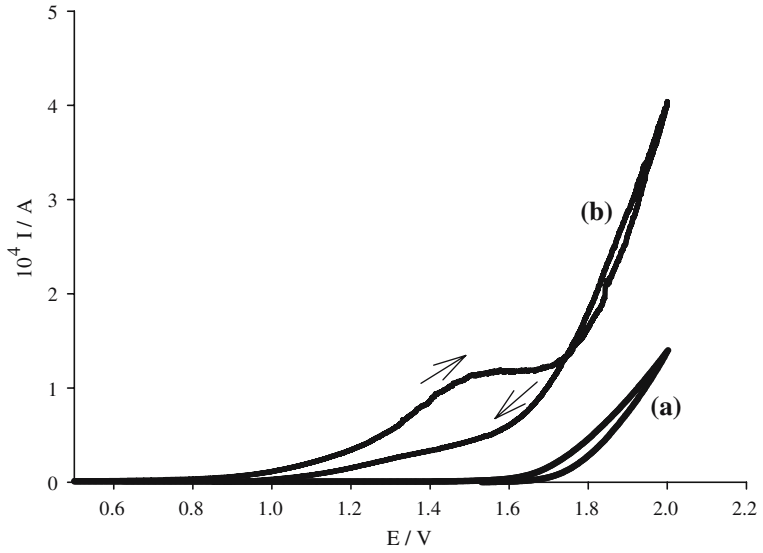

Fig. 1. Cyclic voltammetry of Sb–SnO_2 electrode in 0.1 M Na_2SO_4 (a) and 0.001 M *p*-methoxyphenol + 0.1 M Na_2SO_4 solution (b) at 20 mV s^{-1}.

adsorption, charge transfer and surface reaction. The oxidation rate of PMP was not affected by solution stirring at different rates; thus under the present conditions diffusion of PMP towards the electrode surface is not rate-limiting.

From analysis of solution spectra such as that shown in Figure 2, the composition of solutions during electrolysis at various electrode potentials were obtained and these are shown in Figure 3 as a function of time. The electrooxidation of PMP at 2.0 V (SCE) (Figure 3(a)) produced BQ as the main product accumulated in solution, with generation of only small amounts of CO_2, due to low local concentration of electrogenerated hydroxyl radicals relative to PMP on the anode surface

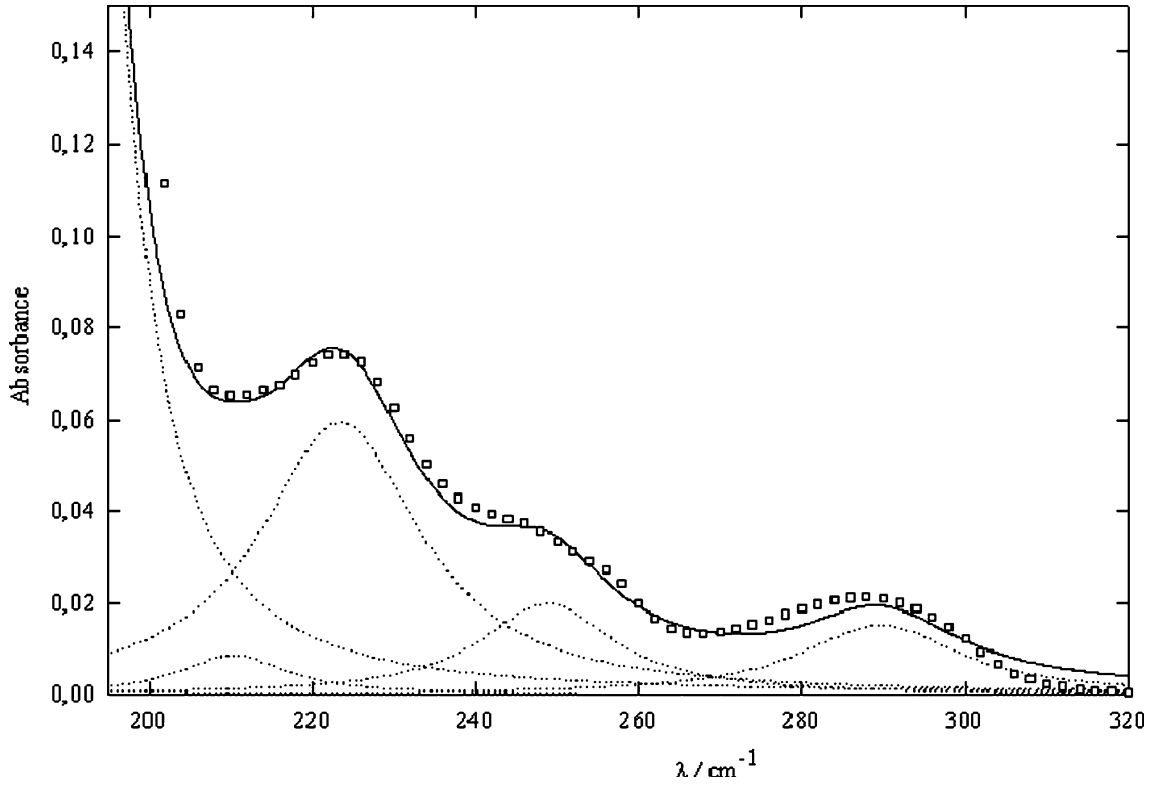

Fig. 2. Intensities of experimental (□□□) and deconvoluted (——) absorption bands in 0.001 M *p*-methoxyphenol + 0.1 M Na_2SO_4 solution, as a function of the electric charge passed during electrolysis under stirring at 2.3 V SCE on SnO_2–Sb_2O_3. Bands I, $\lambda_{max} = 288$ nm, and II, $\lambda_{max} = 230$ nm, correspond to *p*-methoxyphenol; band III, $\lambda_{max} = 248$ nm, to p-benzoquinone, and band IV, $\lambda_{max} = 210$ nm, to maleic acid.

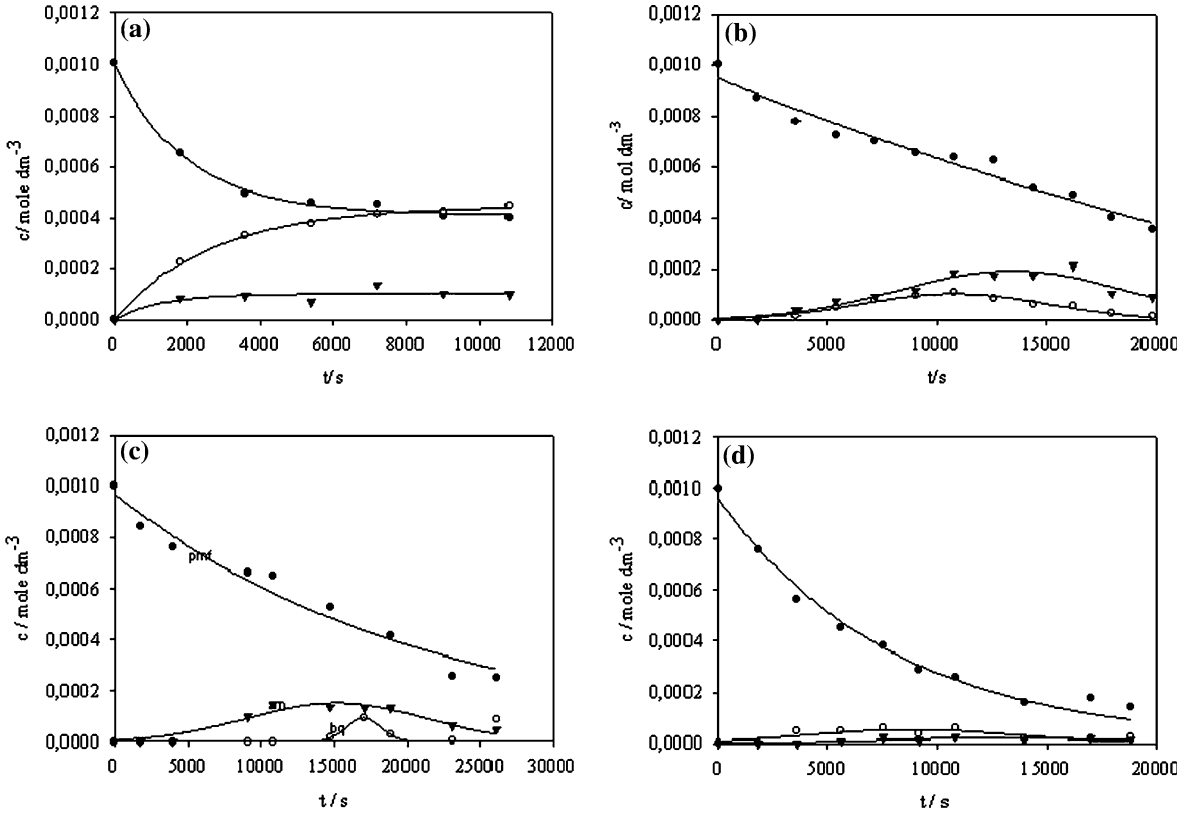

Fig. 3. Concentrations of *p*-methoxyphenol (●), p-benzoquinone (○) and maleic acid (▼) during electrolysis at 2.0 (a), 2.3 (b), 2.5 (c) and 2.65 (d) V (SCE).

[29]. At more positive potentials (Figure 3(b)), the build up of BQ and AA in solution diminished, with corresponding increase in CO_2 generation. At increasingly positive potentials (Figure 3(c) and (d)) the amount of PMP oxidized per unit of circulated electric charge increased, whereas the accumulation of intermediates in solution remained constant, indicating that the availability of active sites for oxidation of PMP on the electrode surface was not affected by generation of $OH^{\bullet}$.

Since BQ is more toxic than PMP [30], oxidation beyond the quinone state is required for environmental applications. Thus from the results shown in Figure 3 and for the purposes of its removal from aqueous solutions, it follows that electrode potentials higher than 2.5 V (SCE) are needed for the removal of PMP by electrooxidation on SnO_2–SbO_2.

PMP as well as all intermediates involved in its mineralization, BQ and AA, are accounted for in the UV-Vis intensities obtained from the spectra. Hence the

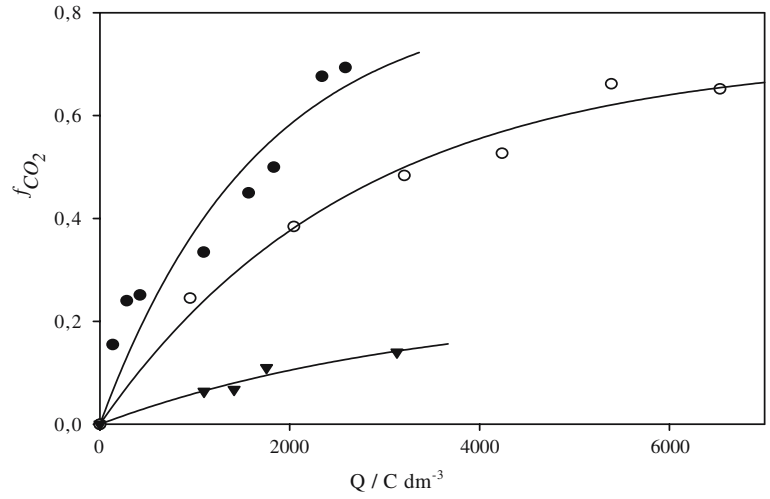

Fig. 4. Fraction of p-metoxyphenol converted to CO_2 (f_{CO_2}) as a function of the electric charge passed, during electrolysis on SnO_2–Sb_2O_3 electrode, under stirring, in 0.01 M p-metoxyphenol + 0.1 M Na_2SO_4 at 2.3 (▼), 2.5 (●), and 2.65 (○) V (SCE).

fraction of organic compound converted to CO_2, f_{CO_2}, may be obtained from the spectral response [27] and is given by the relation,

$$f_{CO_2} = 1 - (c_{PMP} + c_{BQ} + c_{AA})/c_{PMP,0} \quad (5)$$

where c_{PMP}, c_{BQ} and c_{AA} are the concentrations of PMP, BQ and AA at any time of electrolysis, and $c_{PMP,0}$ is the initial concentration of PMP. Figure 4 shows the fraction of organic compound converted to CO_2 as a function of the charge passed through the electrode|solution interface at different electrode potentials. The fraction of organic compound converted to CO_2 increases with the electrode potential up till 2.5 V (SCE). Even though the anodic current continued increasing at more positive potentials, the fraction of PMP converted to CO_2 at a given charge passed decreased continuously at potentials higher than 2.5 V. Thus the increase in the anodic current was primarily due to the increasing rate of the oxygen evolution reaction and the net result was a decline in the Faradaic efficiency for PMP oxidation.

3.2. *Effect of the initial concentration of PMP in solution*

The influence of the initial concentration of phenol on its degradation rate was studied in the concentration range between 0.0001 and 0.1 mol dm^{-3}. Figure 5 shows the concentration of the principal products formed in solution as a function of time, during electrolysis at 2.50 V (SCE) and different initial PMP concentrations. From logarithmic plots of the time-dependence of the PMP concentration (not shown) it follows that the concentration decays with first order kinetics. Figure 5(a) shows that the AA concentration increased up to a maximum at 5.4×10^3 s while the concentration of BQ detected in solution was very low. The increase in concentration of AA in solution observed experimentally and the low concentration of BQ in solution indicate that oxidation of BQ is faster than oxidation of AA. At higher initial concentrations of PMP, accumulation of BQ in solution was enhanced with respect to AA, Figure 5(b) and (c). At concentrations of PMP above 0.1 M the current decreased to low values due to blocking of the electrode surface by deposition of products adhering to the surface. Therefore, removal of BQ from high PMP concentration solutions would be much more difficult and slower, due to the low surface concentration of BQ in the inner Helmholtz layer under these conditions.

Representing the initial PMP oxidation rate as a function of the concentration of PMP in solution, as in Figure 6, shows that the kinetics are well represented by the Langmuir–Hinshelwood mechanism [31], according to which at high PMP concentrations the oxidation rate becomes lower than the adsorption rate and the kinetics become limited by availability of adsorption sites on the electrode surface.

The decaying PMP concentration may also be represented in terms of the rate of the heterogeneous reaction taking place at the metal oxide|solution interface, as

$$dc_{pmp}/dt = kN_0\theta_{OH}\theta_{pmp} \quad (6)$$

where k is the heterogeneous rate constant, N_0 is the number density of adsorption sites on the electrode surface, θ_{OH} is the fractional surface coverage by OH_{ads} arising from the discharge of water, and θ_{pmp} is the fractional surface coverage by pmp_{ads}. Assuming that the fractional surface coverage by OH_{ad} is constant at constant potential, then (6) may be written as

$$dc_{pmp}/dt = k_{app}\theta_{pmp} \quad (7)$$

where the PMP oxidation rate under working conditions depends only on θ_{pmp}. Considering that PMP adsorption fits the Langmuir isotherm as shown in Figure 6, then for reaction times where the principal reaction product is BQ the kinetics may be represented by

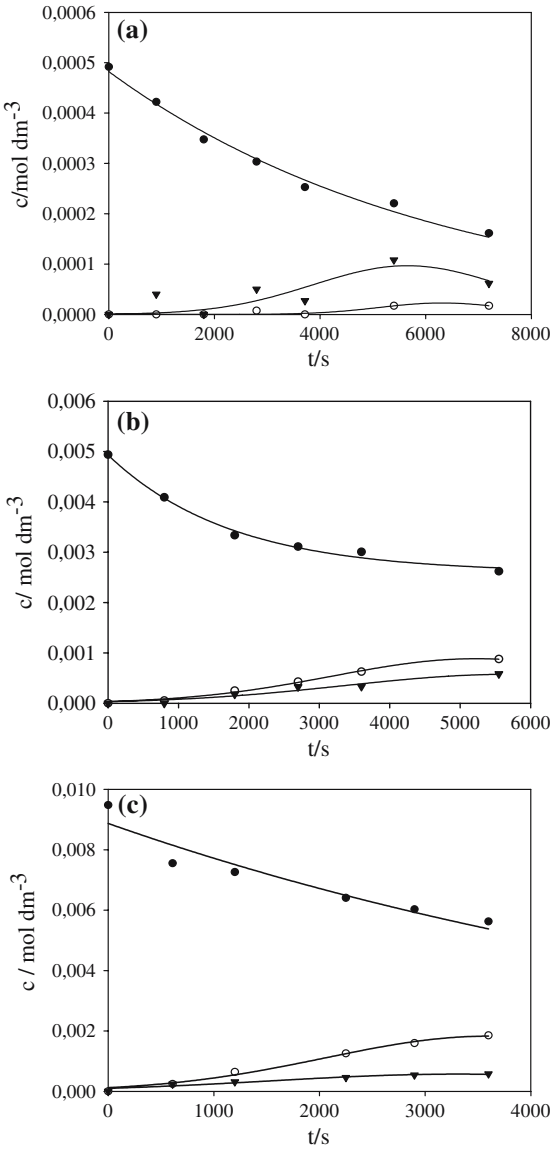

Fig. 5. Concentrations of *p*-methoxyphenol (●), p-benzoquinone (○) and maleic acid (▼) as a function of the charge passed during electrolysis of stirred solutions of 0.01 *p*-methoxyphenol at 2.5 V (SCE) on Sb–SnO_2, with 0.0005 M (a), 0.005 M (b) and 0.01 M (c) *p*-methoxyphenol initially present in solution.

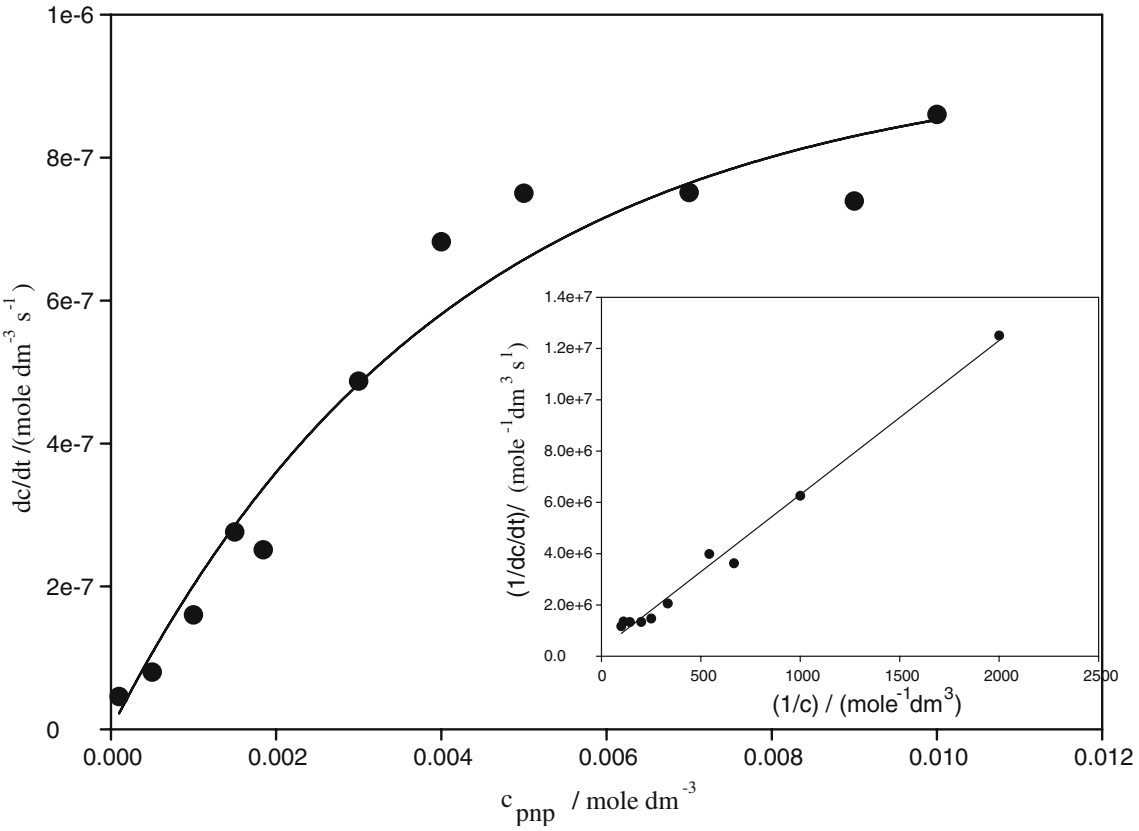

Fig. 6. *p*-methoxyphenol oxidation rates as a function of initial *p*-methoxyphenol concentration in solution; the continuous line indicates the behavior predicted by the Langmuir–Hinshelwood mechanism [29], see text.

$$dc_{PMP}/dt = k_{app}K_{PMP}c_{PMP}/(1 + K_{PMP}c_{PMP} + K_{BQ}c_{BQ}) \quad (8)$$

where K_{PMP} and K_{BQ} are the Langmuir adsorption equilibrium constants for PMP and BQ, respectively. For PMP concentrations far from the surface saturation condition of $\theta_{PMP} = 1$, cf. data shown in Figure 5(a), the decay of PMP concentration was found to be well described at all potentials by linear plots of $\ln(c_{PMP}/c_{PMP,0})$ as a function of electrolysis time, where c_{PMP} is the concentration of PMP at time t and $c_{PMP,0}$ is the initial concentration before electrolysis. Thus PMP electrooxidation follows first order kinetics,

$$dc_{PMP}/dt = k_{app}c_{PMP} \quad (9)$$

where k_{app} is the corresponding apparent rate constant. Integration of (9) yields:

$$-\ln(c_{PMP}/c_{PMP,0}) = k_{app}t \quad (10)$$

Figure 7 shows the time-dependent PMP concentrations and the first order PMP decay rate constants obtained during oxidation of 0.001 M PMP solutions and different BQ concentrations; the PMP oxidation rate constant remained nearly invariant even though the BQ concentrations in solution were varied almost an order of magnitude. This result therefore shows that the PMP surface concentration is not affected by the presence of BQ in solution, thus sustaining the assertion that BQ is displaced from the inner Helmholtz layer upon increasing PMP concentrations in solution.

4. Conclusions

UV–Vis analysis of PMP solutions during electrolysis on Sb–SnO_2 electrodes at different potentials showed increasing oxidation rates at more positive potentials. However the Faradaic efficiency decreased at potentials more positive than 2.5 V (SCE), without affecting the fraction of organic compound oxidized to CO_2. It has been shown that increasing the initial concentration of PMP in solution favours accumulation of BQ and MA intermediates, and that this diminishes the fraction of organic compound oxidized to CO_2, due to exclusion of the electrogenerated BQ from the inner Helmholtz layer.

Acknowledgements

We are grateful to Universidad Simón Bolívar and FONACIT for financial support, also to Michele Milo for managerial and technical assistance and the members of the Electrochemistry Group at USB for discussions.

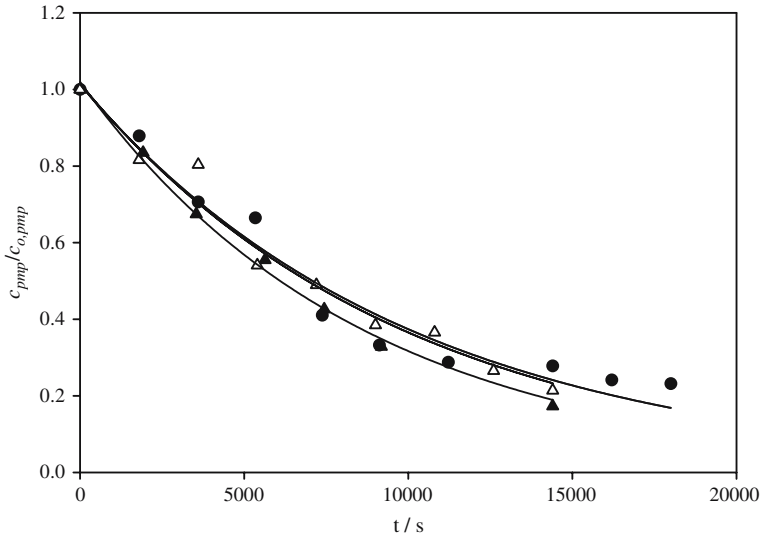

Fig. 7. Decaying *p*-methoxyphenol concentrations as a function of time during electrolysis of 0.001 M *p*-methoxyphenol solutions in the initial presence of 0.00025 (▼), 0.0006 (●), and 0.0007 (○) M benzoquinone.

References

1. H.D. Sharifian and D.W. Kirk, *J. Electrochem. Soc.* **133** (1986) 921.
2. M. Gattrell and D.W. Kirk, *J. Electrochem. Soc.* **140** (1993) 1534.
3. Ch. Comninellis and C. Pulgarin, *J. Appl. Electrochem.* **23** (1993) 108.
4. B.J. Hwang and K.L. Lee, *J. Appl. Electrochem.* **26** (1996) 153.
5. M. Gattrell and D.W. Kirk, *J. Electrochem. Soc.* **140** (1993) 903.
6. D. Popovic and D.C. Johnson, *Anal. Chem.* **70** (1998) 468.
7. N.B. Tahar and A. Savall, *J. Appl. Electrochem.* **29** (1999) 277.
8. D.C. Jonhson, J. Feng and L.L. Houk, *Electrochim. Acta* **46** (2000) 323.
9. A.M. Polcado, S. Palmas, F. Renoldi and M. Mascia, *Electrochim. Acta* **46** (2000) 389.
10. S. Stucki, R. Kozt, B. Carcer and W. Sutter, *J. Appl. Electrochem.* **21** (1991) 99.
11. B. Fleszar and J. Ploszynska, *Electrochim. Acta* **30** (1985) 31.
12. Ch. Comninellis and C. Pulgarin, *J. Appl. Electrochem.* **21** (1991) 703.
13. J.E. Vitt and D.C. Jonhson, *J. Electrochem. Soc.* **139** (1992) 774.
14. K. Jüttner, U. Galla and H. Schmieder, *Electrochim. Acta* **45** (2000) 2575.
15. M.S. Ureta-Zañartu, P. Bustos, M.C. Diez, M.L. Mora and C. Gutierrez, *Electrochim. Acta* **46** (2001) 2545.
16. J. Iniesta, P.A. Michaud, M. Panizza, G. Cerisola, A. Aldaz and Ch. Comninellis, *Electrochim. Acta* **46** (2003) 3573.
17. A.M. Polcaro, A. Vacca, S. Palmas and M. Mascia, *J. Appl. Electrochem.* **33** (2003) 885.
18. L. Codognoto, S.A.S. Machado and L.A. Avaca, *J. Appl. Electrochem.* **33** (2003) 951.
19. M.A. Rodrigo, P. Michaud, I. Duo, M. Panizza, G. Cerisola and Ch. Comninellis, *J. Electrochem. Soc.* **148** (2001) D60.
20. P. Cañizares, J. Garcia-Gomez, C. Saez and M.A Rodrigo, *J. Appl. Electrochem.* **33** (2003) 917.
21. P. Cañizares, J. Garcia-Gomez, J. Lobato and M.A. Rodrigo, *Ind. Eng. Chem. Res.* **42** (2003) 956.
22. J.D. Roogers, W. Jedral and N.J. Bunce, *Environ. Sci. Technol.* **33** (1999) 1453.
23. N.B. Tahar and A. Savall, *J. Electrochem. Soc.* **145** (1998) 3427.
24. O. Simond, V. Schaller and Ch. Comninellis, *Electrochim. Acta* **42** (1997) 2009.
25. G. Foti, D. Gandini, Ch. Comninellis, A. Perret and W. Haenni, *Electrochem. Solid State Lett.* **2** (1999) 228.
26. Ch. Comninellis, *Electrochim. Acta* **39** (1994) 1857.
27. C. Borras, T. Laredo, J. Mostany and B.R. Scharifker, *Electrochim. Acta* **49** (2004) 641.
28. C. Borras, T. Laredo and B.R. Scharifker, *Electrochim. Acta* **48** (2004) 2775.
29. J. Iniesta, P.A. Micahud, M. Pamizza, G. Cerisola, A. Aldaz and Ch. Comninellis, *Electrochim. Acta* **46** (2001) 3573.
30. Z. Wu and M. Zhou, *Environ. Sci. Technol.* **35** (2001) 2698.
31. M.R. Hoffman, S.T. Martin, W. Choi and D.W. Bahnemann, *Chem Rev.* **95** (1995) 69.